NUMERICAL INVESTIGATION OF THE LONG-TIME EVOLUTION AND INTERACTION OF LOCALIZED WAVES

C. I. CHRISTOV *†
Servicio de Predicción Numérica, Instituto Nacional de Meteorología
Paseo de las Moreras, s/n, 28040, Madrid, SPAIN

ABSTRACT

Numerical schemes for two distinct $(1+1)D$ models of free–surface flows are developed. The first class comprise the dissipationless Hamiltonian models featured by the Boussinesq equation. For them a new, fully implicit scheme is devised and shown to conserve within the round-off error of computations the mass, energy and pseudomomentum of the system. The long–time evolution and interaction between localized solutions of type of *sech* (Boussinesq solitons) are investigated. Under certain conditions the *seches* transform into pulses that experience "red–shift" with time. Despite their "aging" nature these pulses are shown to comply with the definition of a soliton since they preserve their identity (shapes) and the total energy of the system is conserved.

The second class considered includes the intrinsically dissipative models (featured here by the KdV–KSV equation). In this case the role of individualized objects (coherent structures) is played by the kink–type solutions (hydraulic jumps, shocks). It is found that the collisions between the coherent structures of KdV–KSV is ideally inelastic in the sense that after the encounter two structures stick to each other forming a structure of larger amplitude (*mass*), the latter evolving in strict compliance with the laws of conservation of *mass* and *momentum* of the wave system.

1. Introduction

A variety of continuous systems are modelled by Nonlinear Evolution Equations (*NEE*) the latter being *PDE* containing the first or second time derivative of the unknown function and spatial and mixed derivatives of different orders. With respect to the spatial variables the *NEE* can be one-, two- or three-dimensional, respectively. The strict description of any physical process is three-dimensional but it is not always tangible for investigation and for this reason a plethora of simplified one-dimensional *NEE* have been recently derived and thoroughly investigated.

*Present address: Instituto Pluridisciplinar, Universidad Complutense, Paseo Juan XXIII, No 1, 28040, Madrid, SPAIN
†On leave from the National Institute of Meteorology & Hydrology, Bulgarian Academy of Sciences, Sofia 1184, BULGARIA

FLUID PHYSICS, LECTURE NOTES OF SUMMER SCHOOLS
M. G. Velarde and C. I. Christov, eds., World Scientific, 1994.

One of the most outstanding features of *NEE* is that under certain conditions the nonlinear, dispersive and dissipative (if present) effects balance each other and localized solutions of type of stationary propagating waves (solitary waves) take place. Borrowing a coinage from the field of turbulence we call the localized solutions "coherent structures". The importance of the coherent structures stems from the fact that they can retain their individuality for considerably longer time intervals than the characteristic times of the small-scale disturbances. Studying their shapes and dynamics can provide a crucial insight into the properties of the particular system under consideration.

The present work is devoted to developing numerical schemes and algorithms for investigation of wave regimes for different *NEE* arising when capillary flows in thin liquid layers are modelled. We concern ourselves with the Proper Boussinesq equation (*PB* – for brevity) and so called Korteweg-de Vries – Kuramoto-Sivashinsky-Velarde equation (*KdV-KSV* for brevity) which are applicable to surface-tension driven capillary waves as well as to internal waves in shear flows. Mathematically speaking the two *NEE* under consideration are of radically different nature. The first one is intrinsically elastic – a generalize wave equation – arising also in the nonlinear elasticity and lattice dynamics and nonlinear dynamics of rods. The second is intrinsically dissipative – a generalized parabolic equation.

The essentially elastic *NEE* – the *KdV* – was the first to undergo a numerical investigation [1] exhibiting particle-like behaviour of the localized solutions. Recently a variety of conservation properties have been proved and analytical techniques developed for the solitary waves [2]. Unfortunately, these analytical techniques do not actually advance much beyond the territory of *sechs*. Furthermore, the solutions of *NEE* are never unique, and there are many more complications arising with any particular *NEE*. One that we try to answer here for the Proper Boussinesq *PB* equation is whether the *sechs* shapes have an appreciable basin of attraction. To tackle this problem we MUST develop for *PB* a fully implicit and *conservative* scheme.

The intrinsically dissipative systems of fluid origin pose a completely different case. With no slight intended to the usual analytical techniques, it is clear that they can not describe as well, or at all, the interaction among coherent structures of dissipative systems as they did for the above mentioned essentially elastic equations. First of all, analytical solutions for the coherent structures that are stationary in the moving frame are found only for isolated values of celerity as a matter of accident [3,4,5]. Yet the thorough investigation of the interaction one needs the shape of a coherent structure for an arbitrary value of the celerity. This goal can only be achieved numerically for a dissipative system. However, this leads to another obstacle since the respective numerical problem is in fact an inverse one due to the very shape of the coherent structure being instable (in most of the cases – metastable). Basing upon the previously developed technique called Method of Variational Imbedding (*MVI*) [6,7] we succeeded in calculating [8] the shapes of different coherent structures with high accuracy. This provided the basis for investigating their interactions in the present work.

We develop here a strongly implicit difference scheme for the *KdV-KSV* equa-

tion with second order spatial approximation and third order temporal approximation. Different conditions at the boundaries of computational domain were tested: "clamped ends", reflecting boundaries, etc. In practice large enough computational domains were used and the particular type of the boundary condition did not affect the development of the coherent structures when they were safely away from the boundaries. The initial condition for the scheme was composed by the superposition of the shapes of two or more coherent structures calculated previously by means of *MVI*. The scheme appears to be numerically stable even for very large time increments. The time increments were only limited by the considerations connected with the approximation.

An extensive set of numerical experiments is conducted and the interactions of different coherent structures are analyzed. The most important findings of the present work are that

1. The collisions of *sech*-solitons in *PB* are elastic only for celerities closer than 1% to the characteristic speed.

2. For arbitrary initial conditions (e.g., *seches* of opposite amplitude) or for initial *sech*-shapes of celerities that do not satisfy 1 the evolution of the solution invariably yields to a *pulse*-like solution that exhibit a kind of self-similar behaviour in the sense that its amplitude decreases and its support increases with time. The *mass* and *pseudoenergy*, however, are perfectly conserved within the round-off error of calculations with double precision.

3. The interactions of the coherent structures of kink-type in *KdV–KSV* are completely inelastic in the sense that after a collision two solitary waves stick to each other forming a new wave with an amplitude corresponding to the sum of the amplitudes of the original waves.

2. The Intrinsically Elastic NEE: Featuring PB

Boussinesq equation was derived [9,10] (see, also [12]) for shallow water flows but it turned out to be improper (see, e.g., [13]), incorrect in the sense of Hadamard. It goes well beyond the scope of present work to discuss the reasons for this apparent failure of the Boussinesq model of flow in shallow layers. It suffices only to mention that in our opinion a correct way to overcome this incorrectness is to apply the idea of so-called Regularized Long-Wave (*RLW*) approximation originated in [14]. We will treat numerically the *RLW* case elsewhere. We are concerned here with the capillary flows where if a sufficiently strong surface tension is included into considerations, then the sign of the fourth spatial derivative changes and Boussinesq equation becomes a higher-order wave equation, namely

$$u_{tt} = [\gamma^2 u + \alpha u^2 - \beta u_{xx}]_{xx} , \qquad \beta > 0 , \tag{1}$$

where $\beta = -\frac{1}{3} + \frac{\sigma}{\rho h_0^2}$. For weak surface tension ($\sigma < \frac{1}{3}\rho h_0^2$), the coefficient β has the improper sign. We are concerned in what follows only with the case $\beta > 0$, which

is referred in the literature as the "good", "proper", etc. We shall call it for brevity *PB*.

2.1. The Formulation as a System. Conservation Laws

Following [15,16] we show in this subsection the conservative formulation of *PB*. The only difference is that while [15,16] are concerned with infinite intervals we consider a finite spatial interval which is the case in numerical implementations. Upon introducing into eq.(1) the auxiliary function w through the relation

$$u_t = w_x \ , \tag{2}$$

and integrating once with respect to x yields

$$w_t = [\gamma^2 u - \frac{dU(u)}{du} - \beta u_{xx}]_x \ , \tag{3}$$

where $U(u)$ is a general notation for the potential (here we have $U(u) = -\frac{\alpha}{3}u^3$). The integration constant in the last equation is set equal to zero. This does not loose generality since an arbitrary function of time can be included in w without changing the definition (2).

The system (2), (3) admits conservation laws iff the following boundary conditions (b.c. – for brevity) are imposed

$$u = 0 \ , \quad w = 0 \qquad \text{for} \qquad x = -L_1, L_2 \ , \tag{4}$$

where $-L_1, L_2$ are the values of spatial coordinate at which the domain is truncated. The shape of a localized solution approaches at each infinity a constant and hence all its derivatives decay automatically to zero. Then when treating the problem analytically one may also impose b.c. on the second, third, etc. derivatives that follows from the condition for decay. These are called asymptotic b.c. However, in numerics and in physics as well, one never has a truly infinite domain and the exact form of the b.c. is of crucial importance. In fact, any conservation or balance law is a property of the boundary value problem (b.v.p) as a whole and not only of the equation itself.

Also, the second of the conditions (4) has as a corollary, the following b.c.

$$[\gamma^2 u - \frac{dU(u)}{du} - \beta u_{xx}]_x = 0 \qquad \text{for} \qquad x = -L_1, L_2 \ .$$

Consider now the quantities

$$A \stackrel{\text{def}}{=} \int_{-L_1}^{L_2} u dx \ , \quad M \stackrel{\text{def}}{=} \int_{-L_1}^{L_2} uw dx \ , \quad E \stackrel{\text{def}}{=} \int_{-L_1}^{L_2} \frac{1}{2}[\gamma^2 u^2 + w^2 + 2U(u) + \beta u_x^2] dx \ . \tag{5}$$

Integrating (2) with respect to x and acknowledging the appropriate b.c from (4) we get that

$$\frac{dA}{dt} = 0 \,, \tag{6}$$

which can be called a conservation law for the *mass* of wave.

Upon multiplying (2) by w and (3) by u, adding them to each other and integrating with respect to çx one obtains the balance law for the quantity M, namely

$$\frac{dM}{dt} = [\frac{1}{2}u_x^2]\Big|_{-L_1}^{L_2} \equiv F \,. \tag{7}$$

Following [17,18] we call M *pseudomomentum*, and F – *pseudoforce*. Although in [17] a quantity similar to E is called energy, we prefer to use the safer coinage *pseudoenergy* because when the Boussinesq equation is of fluid-dynamics origin, E from (5) is not positive definite functional and may not be always interpreted as the energy in the usual sense (i.e., as the energy of the material particles of the fluid) as it is the case of the elasticity applications envisaged in [17].

Finally, upon multiplying (2) by $[\gamma^2 u - \frac{dU(u)}{du} - \beta u_{xx}]$ and (3) by w, adding them up and integrating with respect to x we obtain:

$$\frac{dE}{dt} = 0 \,. \tag{8}$$

The conservation laws (6)– (8) secure that the *mass* and the *pseudoenergy* remain constant during the evolution of the solution. For the case of asymptotic b.c. the balance law (7) suffices to claim that the *pseudomomentum* remains constant as well. Numerically speaking, however, the b.c. are not asymptotic and it may happen that $u_x \neq 0$ at the actual infinities. Only for strictly symmetric evolution, is the *pseudomomentum* conserved after a full cycle of reflections from the boundaries $x = -L_1, L_2$.

Before proceeding with the constructing of the difference scheme, for convenience the system rendered into more symmetric form. For this reason we introduce still another auxiliary function

$$w \equiv q_x \,, \tag{9}$$

and integrate (3) with respect to x. Once again, in taking the respective integration constant equal to zero no generality is lost, since an arbitrary function of time can be incorporated into the definition (9) of q in order to absorb the said constant. Thus one arrives at the following system

$$u_t = q_{xx} \,, \qquad q_t = \gamma^2 u + \alpha u^2 - \beta u_{xx} \,,$$

where α is the coefficient of nonlinear term. In the present paper we consider only the case of quadratic nonlinearity because of its relevance to fluid problems. It is to be emphasized, however, that any other kind of algebraic nonlinearity (cubic, quintic, etc.) can be treated in absolutely the same manner as in what follows.

The boundary conditions (4) adopt the form

$$u = 0\ , \quad q_x = 0 \qquad \text{for} \qquad x = -L_1, L_2\ .$$

2.2. The Conservative Difference Scheme

Let us introduce a regular mesh in the interval $[-L_1, L_2]$ with spacing h, i.e.,

$$x_i = -L_1 + (i-1)h\ , \qquad h = \frac{L_1 + L_2}{N-1}\ , \tag{10}$$

where N is the total number of grid points in this interval. We define the set function $u_i \overset{\text{def}}{=} u(x_i)$.

When the *NEE* under consideration possesses conservation laws, it is desirable is to have them reproduced by the numerical scheme. In this sub-section we construct an implicit difference scheme which conserves the *mass* and *pseudoenergy*.

We leave the problem of linearization for the next sub-section and show first the strictly conservative scheme which is inevitably nonlinear, namely

$$\begin{aligned}\frac{q_i^{n+1} - q_i^n}{\tau} &= \gamma^2 \frac{u_i^{n+1} + u_i^n}{2} + \alpha \frac{(u_i^{n+1})^2 + u_i^{n+1} u_i^n + (u_i^n)^2}{3} \\ &\quad - \frac{\beta}{2}\left[\frac{u_{i+1}^{n+1} - 2u_i^{n+1} + u_{i-1}^{n+1}}{2h^2} + \frac{u_{i+1}^n - 2u_i^n + u_{i-1}^n}{2h^2}\right]\ ,\end{aligned} \tag{11}$$

$$\frac{u_i^{n+1} - u_i^n}{\tau} = \frac{1}{2}\left[\frac{q_{i+1}^{n+1} - 2q_i^{n+1} + q_{i-1}^{n+1}}{h^2} + \frac{q_{i+1}^n - 2q_i^n + q_{i-1}^n}{h^2}\right]\ . \tag{12}$$

with b.c.

$$u_N^{n+1} = u_1^{n+1} = 0\ , \quad q_N^{n+1} - q_{N-1}^{n+1} = q_2^{n+1} - q_1^{n+1} = 0\ . \tag{13}$$

First we prove that if the set functions ϕ_i and ψ_i satisfy the boundary conditions

$$\phi_N - \phi_{N-1} = 0\ ,\ \psi_N - \psi_{N-1} = 0 \qquad \text{and} \qquad \phi_2 - \phi_1 = 0\ ,\ \psi_2 - \psi_1 = 0\ .$$

then

$$\begin{aligned}\sum_1^{N-1} (\phi_{i+1} - \phi_i)^2 &\equiv -\sum_1^{n-1} (\phi_{i+1})^2 + 2\sum_1^{N-1} (\phi_{i+1}\phi_i) + \sum_1^{N-1} (\phi_i)^2 \\ &= \sum_2^{N-1} (\phi_{i+1} - 2\phi_i + \phi_{i-1})\phi_i + \phi_N(\phi_N - \phi_{N-1}) + \phi_1(\phi_2 - \phi_1) \\ &= \sum_2^{N-1} (\phi_{i+1} - 2\phi_i + \phi_{i-1})\phi_i\ .\end{aligned} \tag{14}$$

Respectively,

$$\begin{aligned}\sum_{2}^{N-1}[(\psi_{i+1}-2\psi_i+\psi_{i-1})\phi_i &- (\phi_{i+1}-2\phi_i+\phi_{i-1})\psi_i] \\ &= \phi_{N-1}\psi_N-\phi_N\psi_{N-1}+\phi_2\psi_1-\phi_1\psi_2 \\ &= \phi_N\psi_N-\phi_N\psi_N+\phi_1\psi_1-\phi_1\psi_1=0\,.\end{aligned} \tag{15}$$

Now we are prepared to prove the following

Theorem: The difference approximations of the *mass* and *pseudoenergy*

$$\mathcal{A}=\sum_{i=2}^{N-1}u_ih\,,\quad \mathcal{E}=\sum_{i=2}^{N-1}\Big(\frac{\gamma^2u_i^2}{2}-\frac{\alpha u_i^3}{3}\Big)h+\frac{1}{2}\sum_{i=1}^{N-1}\Big[\beta\Big(\frac{u_{i+1}-u_i}{h}\Big)^2+\Big(\frac{q_{i+1}-q_i}{h}\Big)^2\Big]h\,, \tag{16}$$

are conserved by the difference scheme (11)–(12) in the sense that

$$\mathcal{A}^{n+1}=\mathcal{A}^n \qquad \text{and} \qquad \mathcal{E}^{n+1}=\mathcal{E}^n\,. \tag{17}$$

Proof: After acknowledging the b.c. (13) we obtain from (12) that

$$\begin{aligned}\frac{1}{\tau}\Big(\sum_{2}^{N-1}u_i^{n+1}h &- \sum_{2}^{N-1}u_i^nh\Big)=\frac{1}{2h}\sum_{2}^{N-1}(q_{i+1}^{n+1}-2q_i^{n+1}+q_{i-1}^{n+1}+q_{i+1}^n-2q_i^n+q_{i-1}^n) \\ &= \frac{1}{2h}[q_N^{n+1}-q_2^{n+1}+q_1^{n+1}-q_{N-1}^{n+1}+q_N^n-q_2^n+q_1^n-q_{N-1}^n]=0\,,\end{aligned}$$

which is nothing else but the first of the equalities (17).

Upon multiplying the l.h.s of (11) by the r.h.s of (12) and r.h.s of (11) by the l.h.s of (12), taking the sum between the limits $2, N-1$, and acknowledging (14), (16) we obtain

$$\begin{aligned}\sum_{1}^{N-1}\Big[\frac{1}{2}\frac{(q_{i+1}^{n+1}-q_i^{n+1})^2}{h}+\frac{\beta}{2}\frac{(u_{i+1}^{n+1}-u_i^{n+1})^2}{h}\Big]+\sum_{2}^{N-1}\Big[\frac{\gamma^2}{2}\frac{(u_{i+1}^{n+1})^2}{h}+\frac{\alpha}{3}\frac{(u_{i+1}^{n+1})^3}{h}\Big] \\ = \sum_{1}^{N-1}\Big[\frac{1}{2}\frac{(q_{i+1}^{n}-q_i^{n})^2}{h}+\frac{\beta}{2}\frac{(u_{i+1}^{n}-u_i^{n})^2}{h}\Big]+\sum_{2}^{N-1}\Big[\frac{\gamma^2}{2}\frac{(u_{i+1}^{n})^2}{h}+\frac{\alpha}{3}\frac{(u_{i+1}^{n})^3}{h}\Big]\,,\end{aligned}$$

which precisely the second equality of (17). By construction and design the conservative scheme is obviously stable.

2.3. The Linearization

There exist many different ways to linearize the difference scheme (11), (12). The most robust appears to be the simplest one, namely we introduce an inner iteration

(referred by the index k) for the sought quantities according to the scheme

$$\frac{q_i^{n,k}-q_i^n}{\tau}=\gamma^2\frac{u_i^{n,k}+u_i^n}{2}+\alpha\frac{u_i^{n,k}u_i^{n,k-1}+u_i^{n,k}u_i^n+(u_i^n)^2}{3}$$
$$-\frac{\beta}{2}\left[\frac{u_{i+1}^{n,k}-2u_i^{n,k}+u_{i-1}^{n,k}}{2h^2}+\frac{u_{i+1}^n-2u_i^n+u_{i-1}^n}{2h^2}\right], \tag{18}$$

$$\frac{u_i^{n,k}-u_i^n}{\tau}=\frac{1}{2}\left[\frac{q_{i+1}^{n,k}-2q_i^{n,k}+q_{i-1}^{n,k}}{h^2}+\frac{q_{i+1}^n-2q_i^n+q_{i-1}^n}{h^2}\right]. \tag{19}$$

The inner iterations are conducted starting from the initial conditions

$$u_i^{n,0}=u_i^n \qquad \text{and} \qquad q_i^{n,0}=q_i^n\,,$$

and are terminated at certain $k=K$ after the following criterion is satisfied

$$\frac{\max|u_i^{n,K}-u_i^{n,K-1}|}{\max|u_i^{n,K}|}\le 10^{-11}$$

The threshold value 10^{-11} is selected as safe enough from the round-off error 10^{-15} for computations with double precisions. It is important to note that in all cases described bellow the number of iterations K was between four and six. After the inner iterations are converged one obtains, in fact, the solution for the new time stage $n+1$ of the non-linear conservative difference scheme, namely

$$u_i^{n+1}\stackrel{\text{def}}{=}u_i^{n,K}\,.$$

The scheme (18), (19) consists of two conjugated three-diagonal systems. We found out that an efficient way to solve these systems is to render them into a single five-diagonal system for a new set function defined as follows

$$W_{2i-1}=q_i^{n+1}\,,\quad W_{2i}=u_i^{n+1}\,, \tag{20}$$

and to solve this new system for $2N$ unknowns by means of the specialized solver for Gaussian elimination with pivoting developed in [19].

2.4. The sech-Shape Solitons

To draw conclusions from the *KdV* case about the interaction and to generalize them unto *PB* case is strictly incorrect because the *KdV* is derived from the proper (or improper) Boussinesq equation under the assumption that the solution is almost stationary in the moving frame. It is clear that the last requirement is satisfied only when two waves of almost identical celerities are catching up with one another. Naturally, this would take very long time $O|c_1-c_2|^{-1}$ and the motion during the encounter could be considered as quasi-steady from the point of view of the $O(1)$ time

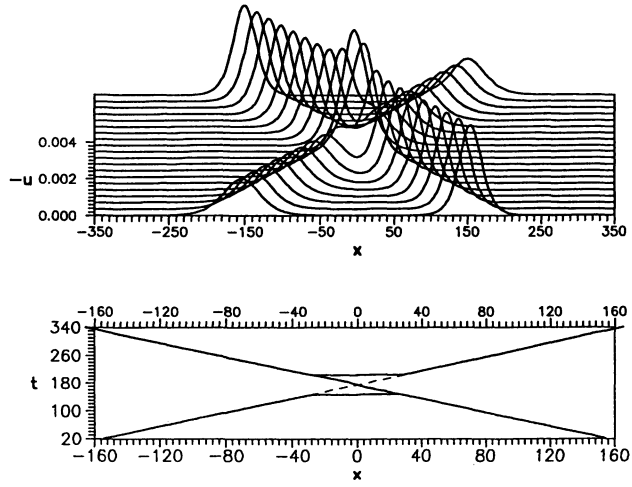

Figure 1: Interaction of two $sech^2$-solitons in PB: $\gamma=1, c_1=0.995,\ c_2=-0.99,\ \Delta t=16.$ Δt is the time difference between two lines of the plot. Ordinate refers to the lowest line. *a)* The shape of the solution; *b)* Trajectories of the "mass-centers".

scale for *PB*. Consequently, the qualitative picture of an encounter (in fact – taking-over collision) of two waves in *KdV* has little in common with the real $O(1)$ clash of two solitons in *PB*. For this reason, our first objective is the head–on collision of two *sechs* that are solutions of *KdV* and of both the "proper" and "improper" Boussinesq equations. For the proper equation (*PB*) the solitons are "subsonic" depressions:

$$u = -\frac{3}{2}\frac{\gamma^2 - c^2}{\alpha}\mathrm{sech}^2\Big(\frac{x}{2}\sqrt{\frac{\gamma^2 - c^2}{\beta}}\Big)\,, \qquad \text{for } |c| < |\gamma|\,, \tag{21}$$

in the sense that the amplitude is negative. Here c is the *celerity* of the wave.

However, there is a subtle difference between *sechs* of *PB* and those of *KdV* which is usually overlooked. In *PB* the swifter waves (with larger celerities) have smaller amplitudes! The case of *KdV* is just the opposite. This is due to the fact that *KdV* is a corollary of *PB* in a moving frame with the characteristic velocity, i.e. the celerity of a *KdV*-soliton is $\sqrt{\gamma^2 - c^2}$, where c is the "absolute" celerity (we call it "absolute" to distinguish from the relative celerity in the moving frame).

In the numerical experiments we set for definiteness $\alpha = -3$, $\beta = 1$, $\gamma = 1$. In Fig. 1-a is presented the head–on collisions of two *sechs*. Different values of the characteristic speed γ can be considered but it is readily shown after re-scaling one arrives at the case $\gamma = 1$. Indeed, this is a good test for the numerical scheme and we did perform calculations with different γ and found that they strictly collapse to the case $\gamma = 1$ after the respective re-scaling. Fig. 1 shows that the soliton interaction is

perfectly elastic. We can only add that the difference approximations $\mathcal{A}$ for the *mass* and $\mathcal{E}$ – for the *pseudoenergy* are conserved in these numerical experiments within an accuracy of order of the round-off error of calculations with double precision, namely 10^{-11}. The *pseudomomentum* is not conserved (and it is not supposed to be) but for the difference approximation of the balance law scaled by the maximum of the solution we obtain a quantity of order of 10^{-12}. As far as the satisfaction of the conservation and balance laws does not depend on the truncation error, we call it "strict in numerical sense". For comparison we mention the works [20,21] where the respective laws are satisfied within 10^{-5}, which though very good is not "strict in numerical sense".

In Fig. 1-b are shown the trajectories of the solitons from Fig. 1-a. It is seen that no phase shift of order of $O(1)$ is observed at the time when [22] provides analytically for phase shift in taking-over collision in *KdV*.

The most important observation of the present work is that the *sechs* persist only for very small deviations from the characteristic speed, namely when

$$0.99\gamma \leq |c| < \gamma\,, \tag{22}$$

which holds true for all characteristic speeds that have been investigated here. The relation (22) appears to be a quantitative assessment of the validity of *KdV* as an approximate equation for calculating the one-way waves of Boussinesq equation‡ As it should have been expected the correspondence between the two equations is valid only in the asymptotic range $O(|\gamma - c|) \ll 1$. It is clear then that the $O(1)$ head–on collisions in *PB* have little in common with the taking–over collisions in *KdV* and the fact that no appreciable phase shift is observed for *PB* in the order $O(1)$ (Figs. 1-b) should not surprise. We did not investigate numerically the taking-over collision of two *sech*-solution in *PB* since the celerities which comply with the limiting case of *KdV* equation differ so slightly from each other in the order $O(1)$, so that it would take large amount of computational time until two *seches* catch up with each other. If larger difference between the celerities is considered then the computational time is reduced, but the requirement for quasi–stationary motion in the moving frame (22) is not satisfied.

In [2,23,24] one finds the conditions on the amplitude of the initial condition under which an initial *sech*-shape transforms into the two-soliton solution (meaning – the two-*sech* solution) of *KdV*. Depending on the initial *mass*, we did, indeed, encounter multi–*sech* solutions in our simulations of *PB*.

Another interesting experiment was suggested in [25]. It consists in taking as an initial condition the same *sech* shape as in (21) but with the opposite (in our case it is positive, in [25] – negative) sign. Then the sech is no more a solution of *PB* and we refer to it as to anti–*sech*. It was interesting to discover that an initial condition of this kind does not transform into a multi–*sech* train, because it is positive amplitude,

‡Be noted that the physical relevance of *BE* is the same as *KdV* since it has been derived [9,10,11] within the same framework of weakly–nonlinear, long–wave approximation and in addition implicit assumption of a right–moving frame was made in [9,10,11].

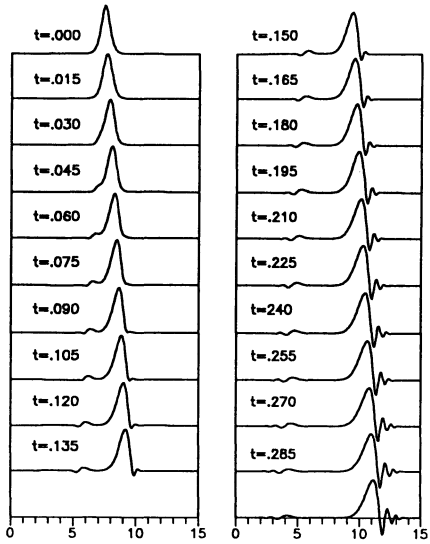

Figure 2: The short-time development of pulses in PB: $\gamma = 10$, when the initial condition is a $sech^2$-solution with celerity $c = 9$.

while the theoretical multi–*sech* solution consists of *seches* of negative amplitude. Our calculations[§] confirmed the finding of [25] that the hump gradually transforms into an oscillatory pulse. We have found that the initial hump broke into two signals that gradually developed into pulses. As the initial celerity of the anti–*sech* is farther from the characteristic speed of the equation, so the process of breaking is fasted. In Fig. 2 is presented the short-time evolution of an anti–*sech* of celerity 0.9γ. A smaller–amplitude signal is emitted in the opposite direction and due to its recoil, the main hump is accelerated to the characteristic speed (becomes a "photon") and then continues its propagation with phase velocity γ. It is to be noted here that even when the initial *sech* has a celerity as low as, say, $c = 0.3\gamma$ the two emerging signals swiftly accelerate to the characteristic speed $c \approx \gamma$ and they continue propagating at that celerity.

2.5. The "Big-Bang" Pulses

It is seen from Fig. 2 that the two pulses into which the initial hump breaks are not stationary creatures. Here we take advantage of the conservativeness of the difference scheme and follow the evolution of the pulse in the moving frame for very

[§]The difference here is that the scheme is conservative and the scenario of generation of a pulse takes place perfectly preserving the *mass* and *pseudoenergy*.

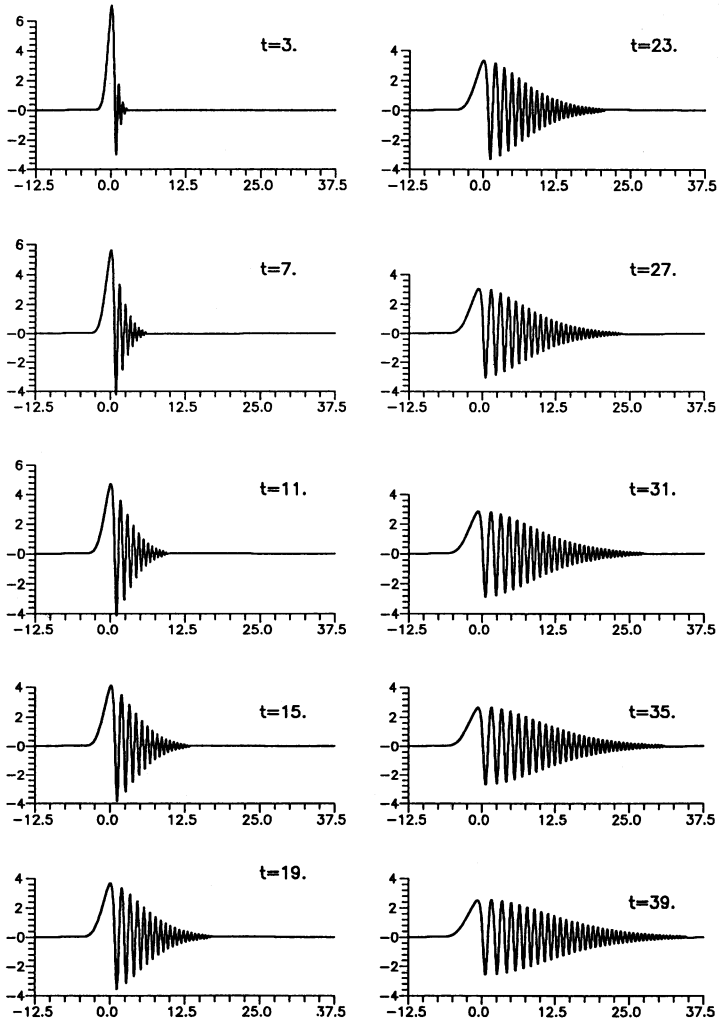

Figure 3: The long-time evolution of the right-going pulse from Fig. 2

long times. In fact, the pulses ware discovered as early as in [23,24] for *KdV* and in [25] for *PB*. Although their existence was reported in [2], they did not attract much attention because of the lack of analytical expression for them. The latter fueled the persistent suspicion that they could be also an artifact of numerics, on one hand, or being essentially linear (the Airy–function shapes) – on the other. Neither of these conjectures appear to be true. One can see that the amplitudes in Fig. 2 are in the nonlinear range. On the other hand the conservativeness of the scheme allows us to claim they are solitons. Fig. 3 shows the long–time evolution of the right–going pulse. Its most important feature is that its amplitude decreases with time while its support increases ("red shift"). This self-similar (we call it also "Big-Bang") behaviour of the pulses of *PB* was observed in our previous calculations [26] with a non-conservative scheme for the case of cubic-quintic nonlinearity. This is an indication that the "Big-Bang" pulses are not an artifact of the numerical scheme. The glimpses of "Big-Bang" behaviour can also be traced back to the relevant numerical calculations for *KdV* (see, the works referred in [2,24]) or for *RLW* (see, [21]), although the time there is not long enough. Insofar as an "one-way" wave is considered in the last case, *PB* reduces to *KdV* and it does not surprise that the self-similar scaling for *PB* found in [26] is the same as the reported in [24,27,28] scaling for *KdV*.

Despite of their "red-shift" appearance the pulses offer a perfect conservation of the *mass* and *pseudoenergy*. We performed experiments on head–on collision of *seches* and discovered that they did preserve their shapes upon collisions, save some "aging" on a time scale much longer than the time scale (cross–section) of collision. Thus they satisfy the main requirements for solitonic behaviour and allow us to call them "aging solitons".

3. The Intrinsically Dissipative NEE: Featuring KdV-KSV

The capillary flow in thin viscous films falling down an inclined plane or vertical wall appears to be a model case for low-dimensional continuous dynamical system. Under the assumption of thin layer, the flow in the bulk can be considered laminar and the influence of the bulk is reduced to the coupled drag force acting upon the surface. As a result an approximate equation containing only the surface variables is derived for the elevation of the free surface. Since the work of Kapitza [29] it is known that the thin-film flow exhibits all major types of behaviour: laminar, periodic and turbulent. The main point here is that the latter is a "surface turbulence" – a chaotic behaviour of the long capillary waves on the surface while the bulk is perfectly laminar and the Poiseuille flow takes place in it. The flow is governed by the Reynolds and Weber numbers,

$$Re = \frac{UL}{\nu}, \qquad We = \frac{\sigma}{\rho g h_0^2}, \tag{23}$$

where σ is the surface tension, ρ – the density, g – the gravity acceleration, h_0 – the thickness of the undisturbed film, ν – kinematic coefficient of viscosity and U is the characteristic velocity. The wave number is defined as the ratio $\alpha = \frac{h_0}{L}$, where L is the characteristic length of the wave under consideration.

Retaining terms up to order $O(\alpha)$ (see [30,31,32,33]) one obtains for the $1D$ waves the following *NEE*:

$$h_t + 2h^2 h_x + (\frac{8}{15} Re h^6 h_x + \frac{2}{3} We h^3 h_{xxx})_x = 0 \ . \tag{24}$$

If the wave number is not large enough, the the term responsible for the surface tension contains geometrical nonlinearities inherent in the expression for the curvature of the surface (see, e.g., [13]). Following [34] where the weakly-nonlinear assumption was consistently appled for the first time, after re–scaling the variables, one obtains

$$\varphi_t + \varphi\varphi_x + \varphi_{xx} + \varphi_{xxxx} = 0 \ , \tag{25}$$

or

$$\psi_t + \psi\psi_x + \psi_{xx} + \psi_{xxxx} = 0 \quad \text{where} \quad \psi_x \equiv \varphi \ . \tag{26}$$

The last form of the *NEE* was also obtained in [35] and for the evolution of reaction fronts – in [3]. Nowadays the eqs.(25), (26) are referred to as Kuramoto-Sivashinsky equation (*KS* for brevity). The only nonlinearity in *KS* is the convective term (called sometimes "eikonal" nonlinearity – [36,37]). When the Marangoni effect is considered on the surface of the thin layer then additional nonlinearity of the form $(\psi\psi_x)_x$ (see [38,39]) appears. The influence on the dynamical behaviour of this additional term as a destabilizing factor (according to its sign in the equation) was elucidated in [36] and the coinage Kuramoto-Velarde equation was introduced. The quantitative effect of the new nonlinearity on the formation of the shapes of the solitary waves was extensively investigated numerically in [7]. In a series of papers, Velarde and co–workers (see [40] and references therein) showed the consistent way of incorporating the Marangoni effects into the one-way long-wave assumption and obtained the following equation

$$u_t + 2\alpha_1 u u_x + \alpha_2 u_{xx} + \alpha_3 u_{xxx} + \alpha_4 u_{xxxx} + \alpha_5 (u u_x)_x = 0 \ , \tag{27}$$

containing also the dispersion term u_{xxx} which is characteristic for the *KdV* model. We call in what follows the eq.(27) Korteweg-de Vries – Kuramoto-Sivashinsky-Velarde equation (*KdV–KSV* – for brevity). For the case of completeness of the review we must mention here that the eq.(27) was considered in many other works (e.g., [4,41,42], etc.) but from the point of view of its mathematical features.

As already mentioned above, the main difference between *PB* and *KdV–KSV* is that the former is intrinsically elastic while the latter is intrinsically dissipative. To be consistent in using the terminology we call *KdV–KSV* generalized parabolic (heat-conduction) equation on the same grounds for calling *PB* generalized hyperbolic (wave) equation. The only difference here is that unlike the standard heat-conduction equation the diffusion in *KdV–KSV* is represented by the fourth spatial derivative while the second spatial derivative and the Marangoni nonlinearity (when with the improper sign) are responsible for a specific pumping of energy. This interplay is characteristic for the long-wave instability of *KS* when the fourth order dissipation fails to bound the second-order pumping. Although apparently simple *KS* possess a rich phenomenology (see [37]).

Since we had thoroughly treated the Marangoni nonlinearity (proportional to α_5) in our previous work [7], here we concentrate mostly on the effects contained in the original *KS* model and in the additional dispersion (proportional to α_3). For this reason we set

$$\alpha_1 = 3 , \qquad \alpha_4 = 1 , \qquad \alpha_5 = 0 .$$

3.1. Coherent structures of KdV–KSV

In the previous case of *PB* we investigated the hump-shaped coherent structures. It was possible because these were stable for certain values of the governing parameters. The most important trait of the intrinsically elastic equations (*PB, KdV, NLS*) is that the hump shapes exist for a continuous spectrum of the celerity. This property and the stability makes them in fact self–preserving (particles) which can move with arbitrary (subsonic) velocity/celerity and whose dynamics are defined by the (meta)dynamics of the respective *NEE*. There is no continuous spectrum, however, for the hump shapes of the intrinsically dissipative equations, such as *KdV–KSV*.

It turned out that a homoclinics (hump shape) exists in *KS* only for a single value of celerity $c = 1.216$ [7,43] although certain papers [41,44,45] suggested that the spectrum could be continuous. A possible explanation of that numerical artifact is offered in [8] which shows that a host of heteroclinics (kink shapes) does exist for a continuous spectrum of celerity. The latter means that for *KdV–KSV* we can investigate the dynamics and interaction of kinks in a similar manner as we did for the humps of *PB*. This is also clear physically because in a dissipative system in order to have a sustained shape one has to pump energy. For the kinks the energy comes from the difference between the surface levels behind and before the wave. The *KdV–KSV* is very similar to Burgers equation where shocks are formed between two stationary states. The energy dissipated in the shock is compensated by the difference of the levels of the solution at left and right infinity ($u_{-\infty}$ and $u_{+\infty}$), respectively.

By definition, a heteroclinic orbit (a kink) is called the localized wave for which:

$$u \overset{x\to-\infty}{\longrightarrow} u_{-\infty} , \quad u \overset{x\to+\infty}{\longrightarrow} u_{+\infty} \quad \text{and} u_{+\infty} \neq u_{-\infty} , \tag{28}$$

When stationary in the moving frame $\xi = x - ct$ waves are considered, then eq. (24) reduces to an *ODE* which can be integrated once to obtain

$$-cu + \alpha_1 u^2 + u' + \alpha_3 u'' + u''' = C_1 ,$$

where the prime stands for a differentiation with respect to ξ. The constant of integration C_1 is defined from the boundary conditions (28). Due to their asymptotic nature they imply that all of the derivatives (which exist) of function u decay at both infinities. Then for the integration constant C_1 we obtain two conditions

$$-cu_{-\infty} + u_{-\infty}^2 = C_1 = -cu_{+\infty} + u_{+\infty}^2 ,$$

which are consistent iff

$$c = \alpha_1(u_{-\infty} + u_{+\infty}) \qquad \text{and} \qquad C_1 = -\alpha_1 u_{-\infty} u_{+\infty} \,. \tag{29}$$

The first analytical kink solution (a combination of hyperbolic tangents) was obtained already in the original work [3]. Unlike the case of *KdV* and *PB*, however, the solution was found only for one single value of the celerity. For the more general equation *KdV–KSV* the same kind of solution was found in [4,23]. Our previous numerical work [8] based on the Method of Variational Imbedding had shown that various kink solutions do exist for all celerities larger than 0.3. For intermediate values of celerity even more than one kink solution appears. The case of lower celerities approaches in fact the limit of linear waves and no localized solutions exist. The results of [8] are crucial for the investigation presented here of the interaction of structures in *KdV–KSV*.

Before turning to the specifics of the numerical implementation it is important to explore further the analogy between the kinks in the dissipative systems and humps in elastic systems. The first spatial derivative of the kink is a standard hump which can be appreciated in a similar manner as the humps of *PB*. In this instance we can call *mass* of the wave the integral of the first spatial derivative (the hump), namely

$$A = \int_{-\infty}^{\infty} \frac{\partial u}{\partial x} dx \equiv u_{-\infty} - u_{\infty}$$

Respectively the momentum of the wave is

$$M \equiv Ac = \alpha_1(u_{-\infty}^2 - u_{\infty}^2) \tag{30}$$

Numerical calculations are not needed to establish the "conservation laws" for the *mass* and *pseudomomentum* of the waves inasmuch as they are a matter of b.c., i.e. it is not necessary now to bear them in mind when constructing the difference scheme because they are satisfied trivially. Yet they have profound physical meaning and define the behaviour of the wave system after the encounter of two waves.

3.2. The Difference Scheme

It is convenient to render (23) into a system of two second-order with respect to spatial variable equations, namely

$$u_t + \alpha_1 u u_x + q + q_{xx} = 0 \,, \tag{31}$$

$$u_{xx} = q \,. \tag{32}$$

In the case of *PB* the formulation as a system had its physical significance since it showed that *PB* can be represented as a Hamiltonian system. In the case of *KdV–KSV* the presentation as a system has only numerical significance because it yields a five-diagonal representation (see (20)). One could argue that the original form

of *KdV–KSV* would have also lead us to a system with five-diagonal matrix, but only of N equations while according to (20) the form (31), (32) is recast into a system of $2N$ equations. The difference is that the finite difference approximation of the system (31), (32) has a matrix whose determinant is of order of $O(h^2)$, while the original formulation – of order of $O(h^4)$. The difference is crucial when large N are considered because the direct method of Gaussian elimination is ill conditioned when the determinant of the matrix is small. Even the theoretically stable Gaussian elimination with pivoting [19] may lose accuracy for $N > 1000$ due to the rounding-off of the numbers in the computer representation when the determinant is too small (say, $O(h^4)$).

The mesh is similar to the case of *PB* (see (10)). The only difference is that the mesh for function q_i is staggered with respect to the main mesh.

Unlike the Boussinesq equation, here no conservation laws are to be satisfied. Then the only requirement for the scheme is to be as much implicit as possible in order to eliminate all numerical instabilities. Since our goal is the long-time evolution, it is preferable to have very high order of approximation with respect to time in order to be able to use large time increments. For this reason we use a four-stage scheme which provides third order of approximation in time. Since a multistage scheme requires more initial conditions than available, at the initial stages it is simply two-stage or three-stage scheme. The latter means that we approximate the time derivative as follows

$$\left.\frac{\delta u}{\delta t}\right|_{i-\frac{1}{2}}^{n+1} \equiv \frac{1}{2}\left[\frac{11u_i^{n+1}-18u_i^n+9u_i^{n-1}-2u_i^{n-2}}{6\tau}+\frac{11u_{i-1}^{n+1}-18u_{i-1}^n+9_{i-1}^{n-1}-2u_{i-1}^{n-2}}{6\tau}\right],$$

$$\left.\frac{\delta u}{\delta t}\right|_{i-\frac{1}{2}}^{2} \equiv \frac{1}{2}\left[\frac{3u_i^2-4u_i^1+u_i^0}{2\tau}+\frac{3u_{i-1}^2-4u_{i-1}^2+u_{i-1}^0}{2\tau}\right],$$

$$\left.\frac{\delta u}{\delta t}\right|_{i-\frac{1}{2}}^{1} \equiv \frac{1}{2}\left[\frac{u_i^1-u_i^0}{2\tau}+\frac{u_{i-1}^1-u_{i-1}^0}{2\tau}\right],$$

Then the difference scheme reads

$$\left.\frac{\delta u}{\delta t}\right|_{i-\frac{1}{2}}^{n+1} + \frac{\alpha_4}{h^2}(q_{i+\frac{1}{2}}^{n+1}-2q_{i-\frac{1}{2}}^{n+1}+q_{i-\frac{3}{2}}^{n+1})+\frac{\alpha_3}{2h}(q_{i+\frac{1}{2}}^{n+1}-q_{i-\frac{3}{2}}^{n+1})+\alpha_2 q_{i-\frac{1}{2}}^{n+1}$$

$$+ 4\alpha_1\frac{u_i^n u_i^{n+1}-u_{i-1}^n u_{i-1}^{n+1}}{h}=2\alpha_1\frac{u_i^{n^2}-u_{i-1}^{n^2}}{h}+O(\tau^3+h^2),$$

$$\frac{1}{h^2}(u_{i+1}^{n+1}-2u_i^{n+1}+u_{i-1}^{n+1})=\frac{1}{2}(q_{i+\frac{1}{2}}^{n+1}+q_{i-\frac{1}{2}}^{n+1}).$$

3.3. Results and Discussion

Let us turn to the results of the direct numerical simulation of the interaction of kinks in *KdV–KSV*. We compose the initial condition from two kinks: the first

(the left) between the levels $u_{left} = u_{-\infty}$, $u_{right} = u_m$; and the second – between $u_{left} = u_m$, $u_{right} = u_{+\infty}$. We start with the dispersionless case.

In Fig. 4-a,b is shown the evolution of a system of two kinks going in the same direction (to the right). To the left is superimposed the kink of larger amplitude. It goes faster and catches up with the kink situated to the right and after a short period of collision they form a single kink proceeding with lesser celerity to the right but containing the same *pseudomomentum* (see (30). This scenario is repeated in Fig. 5-a,b where the two kinks are of equal amplitude. Once again the kink on the left are faster since it is between two higher levels (see (29) for the expression of the celerity). Even when the left kink has a lesser amplitude (Fig. 6-a,b) it goes faster since it is superimposed over the level of the right kink.

In Figs. 4-c,5-c,6-c are shown the trajectories of the "centers" of the coherent structures (kinks). A center of a kink is defined as the point where $u = (u_{left} + u_{right})/2$. According to this definition after the two kinks fuse to form a single, then two different points are referred to as centers. Although very close the trajectories of these two points are different and this is seen in the said figures as two lines that are very close to each other.

Although the interaction is completely inelastic one can see that what can be conserved is indeed conserved and the trajectories exhibit no phase shift. The notion of phase shift, however, needs some clarification in this case. In the figures concerning the trajectories the projections are given of the trajectories the coherent structures would have followed if they were isolated (the dashed lines). The middle dashed line represents the projected trajectory of a single kink (with *mass* that is the sum of the two initial *masses*) and which moves with the celerity pertinent to the conservation of the *pseudomomentum* commencing its motion from the position of the "mass center" of the system of two initial kinks. One sees that after the composite coherent structure (the composite *particle*) is formed in the numerical simulations, it proceeds exactly (within the error of the scheme) alongside the projected trajectory of the so-defined single *particle* containing the total *mass* of the system. In this sense we claim that there is no phase shift in *KS*.

The picture is completely the same if we consider the head–on collision of kinks. In Figs. 7-a,b and 8-a,b is shown the collision without dispersion. Once again the interaction is completely inelastic and there is no phase shift (Figs. 7-c and 8-c). This allows us to use the coinage "ideally inelastic interaction". It is interesting to note that incorporating dispersion ($\alpha_3 \neq 0$) does not change the character of the interaction leaving it ideally inelastic (see Fig. 9). Only the shape of the kink becomes more wavy (see Fig. 10 for better resolution of the initial and final stages of Fig. 9). In Fig. 11 are presented the shapes of single kinks for larger values of dispersion coefficient ($\alpha_3 = 5, 10$). In these two cases the interaction is essentially the same as in Fig. 9,10 and it is not shown here in order not to abuse the size of paper.

In order to especially stress the completely inelastic nature of the interactions among the coherent structures of the intrinsically dissipative system as *KdV–KSV* we prefer to use the coinage **clayons** stemming from the notion that after the collision

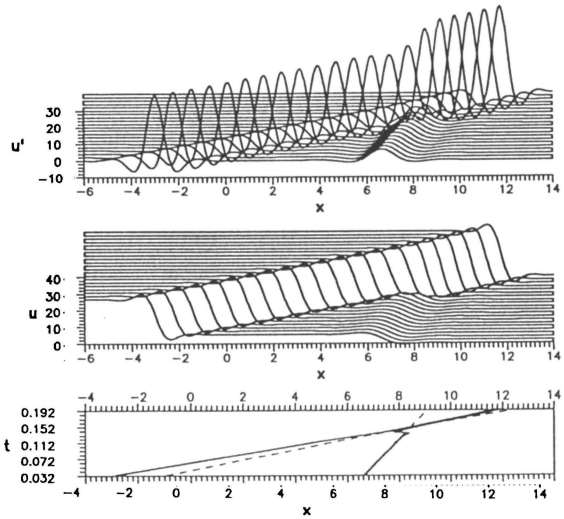

Figure 4: Taking over collision of two *kinks*(*clayons*) in *KS*: $u_{-\infty} = 96/3, u_m = 16/3, u_{+\infty} = 0$

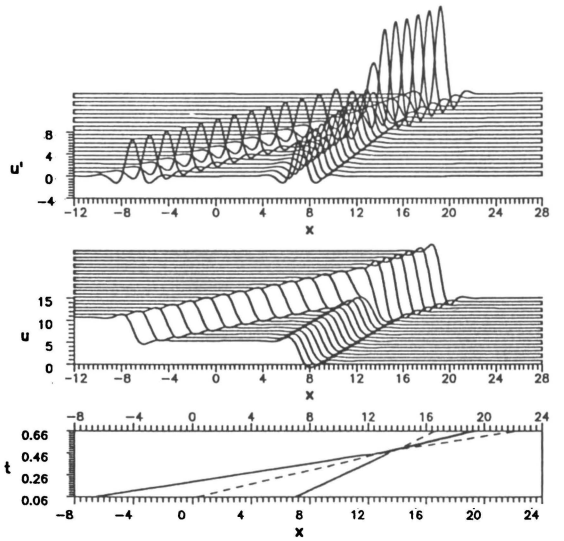

Figure 5: Taking over collision of two *kinks*(*clayons*) in *KS*: $u_{-\infty} = 48/3, u_m = 16/3, u_{+\infty} = 0$

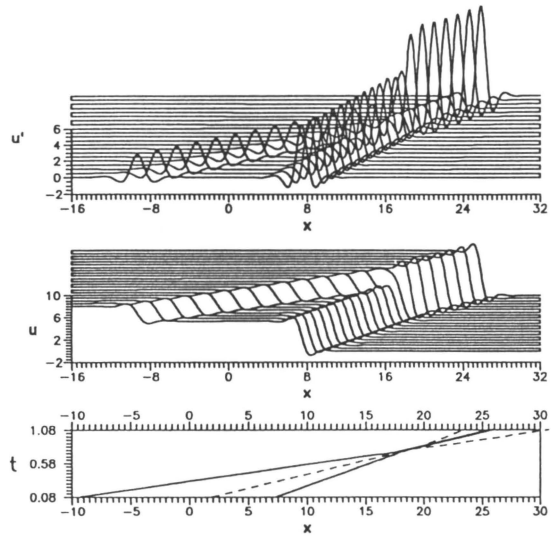

Figure 6: Taking over collision of two *kinks*(*clayons*) in *KS*: $u_{-\infty} = 40/3, u_m = 16/3, u_{+\infty} = 0$

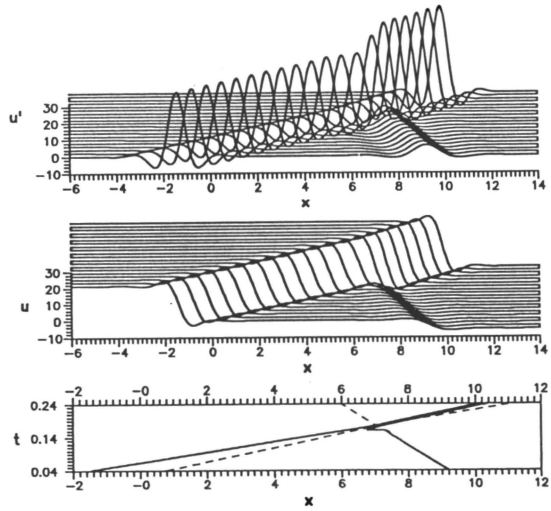

Figure 7: Head–on collision of two *kinks*(*clayons*) in *KS*: $u_{-\infty} = 64/3, u_m = 0, u_{+\infty} = -16/3$

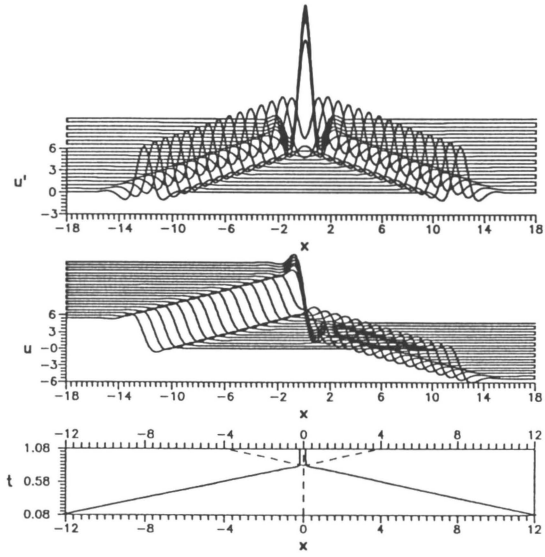

Figure 8: Head–on collision of two *kinks*(*clayons*) in *KS*: $u_{-\infty} = 16/3, u_m = 0, U_{+\infty} = -16/3$

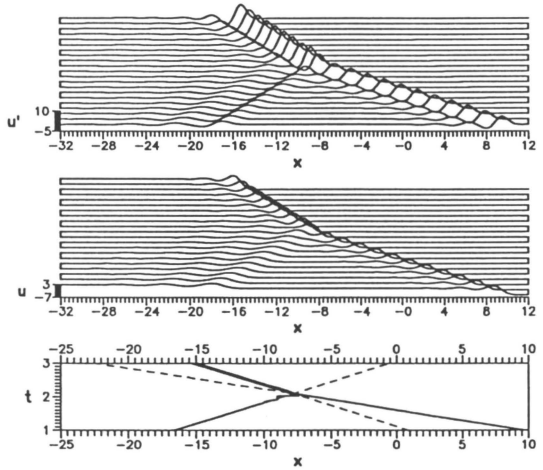

Figure 9: Head–on collision of two *kinks (clayons)* in *KdV-KSV*: $\alpha_1 = 3, \alpha_3 = 3, u_{-\infty} = 8/3, u_m = 0, u_{+\infty} = -16/3$

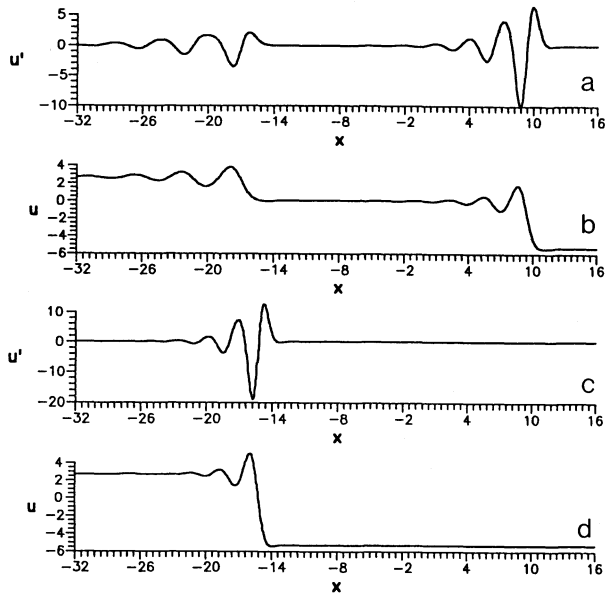

Figure 10: Initial and final stages of the evolution depicted in Fig. 9: *a)* initial shape of the second derivative derivative u_{xx}; *b)* initial shape of the kink u; *c)* final shape of the second derivative derivative u_{xx}; *d)* final shape of the kink u;

two solitary waves of *KdV–KSV* stick to each other as two clay balls.

4. Concluding Remarks

This work presents a precise and carefully developed numerical schemes – adequate research tools in the nonlinear dynamics of coherent structures and solitons.

Implicit schemes for two classes of *NEE* are developed. The first class consists of intrinsically elastic equations (generalized wave equations) that possess conservation laws. The scheme proposed here represents exactly (within the round-off error of the computer) the conservation laws for the *mass* and *pseudoenergy* of wave (system of solitary waves), as well as the balance law for the *pseudomomentum*.

For the case of intrinsically dissipative equations (featuring the so-called *KdV–KSV* equation) when no conservation laws are to be reproduced by the scheme the only preoccupations are the stability and approximation and hence the scheme is four-stage in time and with Newton's quasilinearization of the nonlinear terms. The practical stability of the scheme is virtually unlimited which allowed the pursuit of the very-long time evolution of the solution. We discovered that the interaction of kinks is completely inelastic in the sense that after the collision two kinks of *KS* form

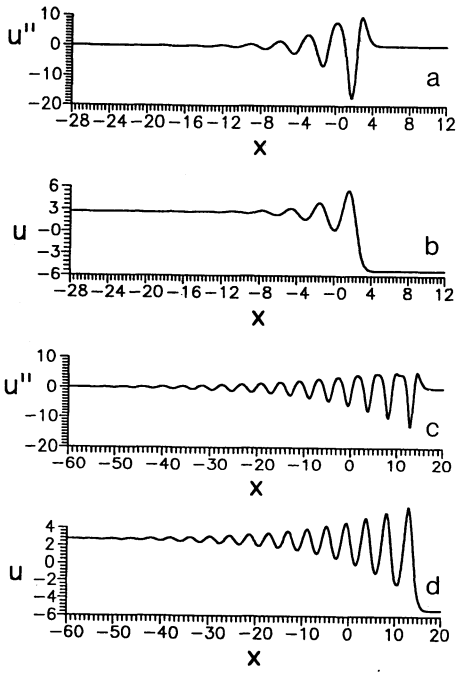

Figure 11: The role of dispersion in forming the shape of the kink in *KdV-KSV*: *a)* the second derivative u_{xx} for $\alpha_3 = 5$; *b)* the second derivative u_{xx} for $\alpha_3 = 10$; *c)* the kink u for $\alpha_3 = 5$; *d)* the kink u for $\alpha_3 = 10$.

a larger kink which proceeds with celerity defined by the conservation of a quantity called *pseudomomentum*.

Acknowledgements

A sabbatical fellowship from the Spanish Ministry of Science and Education is gratefully acknowledged. Author is indebted to Prof. M. G. Velarde for many stimulating discussions.

5. References

1. N. Zabusky, M. D. Kruskal, Interaction of "Solitons" in Collisionless Plasma and the Recurrence of Initial States, *Phys. Rev. Lett.*, **15** (1965) 240–243.
2. P. G. Drazin, R. S. Johnson, *Solitons: an Introduction*, (Cambridge University Press, 1987).
3. Y. Kuramoto, T. Tsuzuki, Persistent Propagation of Concentration Waves in Dissipative Media Far from Thermal Equilibrium, *Progr. Theor. Phys.*, **55** (1976) 356–369.

4. N. A. Kudryashev, Exact Soliton Solutions for a Generalized Equation of Evolution for the Wave Dynamics, *Prikladnaya Math. i Mekhanika*, **52** (1988) 465–470.
5. R. Conte, M. Musette, Penlevé analysis and Bäclund Transformation in the Kuramoto-Sivashinsky Equation, *J. Phys. A: Math. Gen.*, **22** (1989) 169–177.
6. C. I. Christov, A Method for Identification of Homoclinic Trajectories, In: *Proc. 14-th Spring Conf. Union of Bulg. Mathematicians,* Sunny Beach, 6-9.04.1985, (1985) 571–577.
7. C. I. Christov, M. G. Velarde, On Localized Solutions of an Equation Governing Benard-Marangoni Convection, *Appl. Mathem. Modelling*, **17** (1993) 311–320.
8. C. I. Christov, Localized Solutions for Fluid Interfaces via Method of Variational Imbedding, In: *These Proceedings.*
9. J. V. Boussinesq, Théorie de l'intumescence liquide appelé onde solitaire ou de translation, se propageant dans un canal rectangulaire, *Comp. Rend. Hebd. des Seance de l'Acad. des Sci.*, **72** (1871) 755–759.
10. J. V. Boussinesq, Théorie des ondes et des remous qui se propagent le long d'un canal rectangulaire horisontal, en communiquant au liquide contenu dans ce canal des vitesses sensiblement pareilles de la surface au fond, *Journal de Mathématiques Pures et Appliquées*, **17** (1872) 55–108.
11. J. V. Boussinesq, Théorie générale des mouvements qui sont propagés dans un canal rectangulaire horizontal, *Comp. Rend. Hebd. des Seance de l'Acad. des Sci.*, **73** (1871) 256–260.
12. J. Sander, K. Hutter, On the Development of the Theory of the Solitary Wave. A Historical Essay, *Acta Mecanica*, **86** (1991) 111–152.
13. A. Oron, Ph. Rosenau, Formation of Patterns Induced by Thermocapillarity and Gravity, *J. Phys. II France*, **2** (1992) 131-146.
14. D. H. Peregrine, Calculations of the Development of an Undular Bore, *J. Fluid Mech.* **25** (1966) 321-330.
15. V. S. Manoranjan, A. R. Mitchel, J. L. L. Moris, *SIAM J. Sci. Statist. Comput.*, **5** (1984) 946.
16. V. S. Manoranjan, T. Ortega, J. M. Sanz-Serna, Soliton and antisoliton interactions in the "good" Boussinesq equation, *J. Math. Phys.*, **29** (1988) 1964-1968.
17. G. A. Maugin, Application of an Energy-Momentum Tensor in Nonlinear Elastodynamics, *J. Mech. Phys. of Solids*, **29** (1992), 1543–1558.
18. G. A. Maugin, C. Trimarco, Pseudomomentum and Material Forces, in: *Nonlinear Elasticity: Variational Foundation and Application to Brittle Fracture, Acta Mecanica*, **94** (1992), 1–28.
19. C. I. Christov, Gaussian Elimination with Pivoting for Multidiagonal Systems, Internal Report, **4**, University of Reading, 1994.
20. G. A. Gardiner, L. R. T. Gardiner, A. H. A. Ali, Modelling Non-Linear Waves with B-Spline Finite Elements, In: *Mathematical and Numerical Aspects of Wave Propagation Phenomena*, Eds. G. Cohen, L. Halpern, P. Joly, (SIAM,

Philadelphia, 1991), 533-541.
21. G. A. Gardiner, L. R. T. Gardiner, Solitary Waves of the Regularized Long-Wave Equation, *J. Comput. Phys.*, **91** (1990) 441-459.
22. J. M. Miles, Solitary Waves, *Ann. Rev. Fluid Mechanics*, **12** (1980) 11-43.
23. B. Fornberg and G. B. Whitham, A Numerical and Theoretical Study of Certain Nonlinear Wave Phenomena, *Proc. Roy. Soc.* **289** (1978) 373–404.
24. Yu. A. Berezin, *Numerical Investigation of Nonlinear Waves in Rarefied Plasma*, (Nauka, Novosibirsk, 1977) (in Russian).
25. M. P. Soerensen, P. L. Christiansen and P. S. Lohmdahl, Solitary Waves on Nonlinear Elastic Rods I., *J. Acoust. Sos. Am.* **76** (1984) 871–879.
26. C. I. Christov, G. A. Maugin, An implicit difference scheme for the long-time evolution of localized solutions of a generalized Boussinesq system, *J. Comp. Phys.* (1994), to appear, (see also: A Numerical Venture into the Menagerie of Coherent Structures of Boussinesq Equation, In: *Proc. 7th Interdisciplinary Workshop "Nonlinear Coherent Structures in Physics and Biology"*, Dijon, France, 4-6.VI.1991. Eds. Peyrad, M. Remoissenet, Springer, 1991, pp.209-216)
27. A. C. Newell, *Solitons in Mathematics and Physics,* (SIAM, Philadelphia, 1985).
28. G. L. Lamb, *Elements of Soliton Theory*, (Wiley, New York, 1980).
29. P. L. Kapitza, Wave Flow in Thin Layer of Viscous Liquid, *JETF*, **18** (1948) 3-18. (in Russian) (see, also Kapitza & Kapitza, Wave Flow of Thin Layers of a Viscous Fluid, In *Collected Works.* Pergamon, 1965, 690-709.)
30. D. J. Benney, Long Waves in Liquid Film, *J. Maths & Phys.*, **45** (1966) 150-155.
31. S. P. Lin, Finite-Amplitude Side-Band Instability of a Viscous Film, *J. Fluid Mech.*, **63** (1974) 417-429.
32. C. Nakaya, Long Waves on a Thin Fluid Layer Flowing Down an Inclined Plane, *Phys. Fluids*, **18** (1975) 1407-1412.
33. M. V. G. Krishna, S. P. Lin, Non-Linear Stability of a Viscous Film with Respect to Three-Dimensional Side-Band Disturbances, *Phys. Fluids*, **20** (1977) 1039-1044.
34. G. M. Homsy, Model equations for wavy viscous film flow, *Lect. in Appl. Math.*, **15** (1974) 191–194.
35. G. I. Sivashinsky, D. M. Michelson, On Irregular Wavy Flow of a Liquid Film down a Vertical Plane, *Progr. Theor. Phys.*, **63** (1980) 2112-2114.
36. J. M. Hyman, B. Nicolaenko, Coherence and Chaos in Kuramoto-Velarde Equation, In: *Directions in Partial Differential Equations*, (Academic Press, 1987) 89-111.
37. J. M. Hyman, B. Nicolaenco, The Kuramoto-Sivashinsky Equation: A Bridge between PDE's and Dynamical Systems, *Physica*, **18D** (1986) 113-126.
38. P. L. García-Ybarra, J. L. Castillo, M. G. Velarde, *Phys. Fluids*, **30** (1987) 2655.
39. B. K. Kopbosynov, V. V. Pukhnatchev, Thermocapillary Motion in Thin

Liquid Layer, in: *Gidromekhanika i Protzessy Perenosa v Nevesomosti*, Sverdlovsk, 1983 (in Russian) (see, also Kopbosynov & Pukhnatchev, *Fluid. Mech., Sov. Res.*, **13** (1986) 95.)

40. A. N. Garazo, M. G. Velarde, Dissipative Korteweg-de Vries description of Marangoni-Bénard oscillatory convection, *Phys. Fluids*, **A3** (1991) 2295-2300.
41. T. Kawahara, S. Toh, Pulse Interactions in an Unstable Dissipative–Dispersion Nonlinear System, *Phys. Fluids*, **31** (1988) 2103-2111.
42. S.–Y. Lou, G.–X. Huang, X.–Y. Ruan, Exact Solitary Waves in a Convecting Fluid, *J. Phys. A: Math. Gen.*, **24** (1991) L587-L590.
43. O. Yu. Tzvelodub, Stationary Propagating Waves on a Thin Film Falling down a Vertical Wall, In: *Volnovie Protzessy v Dvukhfaznykh Sredakh*, Ed. V. E. Nakoryakov, (Novosibirsk, 1980), 47-63. (in Russian)
44. H.–C. Chang, Evolution of Nonlinear Waves on Vertically Falling Films – A normal Form Analysis, *Chem. Engn. Sci.*, **42** (1987) 515-533.
45. C. I. Christov, V. P. Nartov, Application of the Method of Variational Imbedding for Calculating Shapes of Solitons on Falling Thin Films, In: *Proc. Conf. on Centenary of Academician L. Tchakalov*, (Samokov, Bulgaria, 1986), 135-142. (in Russian)